Moment of fluid method for multimaterial flows

M. Jemison, M. Sussman, M. Shashkov

Department of Mathematics, Florida State University

October 1, 2012

Recent Motivating Work

- Volume preserving Moment-of-Fluid reconstruction for multiple materials. Moment of Fluid method for deforming boundary problems (Ahn and Shashkov, JCP 2007; Ahn and Shashkov, JCP 2009).
- variable density cell centered pressure projection (Kwatra, Su, Gretarsson, Fedkiw 2009)

Laminar jet - density ratio 819:1

X. Li (UTRC), M. Arienti (UTRC), M. Soteriou (UTRC), M. Sussman (FSU).

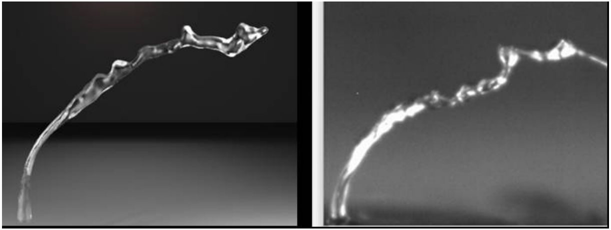

Turbulent jet spray - density ratio 819:1

X. Li (UTRC), M. Arienti (UTRC), M. Soteriou (UTRC), M. Sussman (FSU).

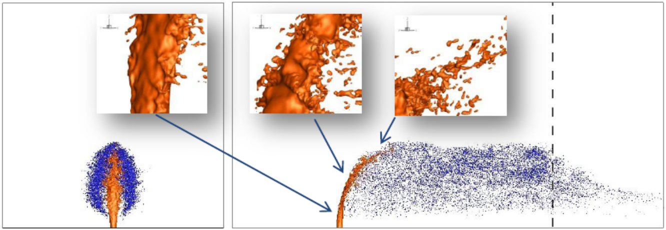

Figure 6. Front (a) and side view (b) of the jet at $t = 1.686$ ms. The jet calculated by CLSVOF on the Eulerian grid is represented by the rendering of the 0 level set iso-surface. The spray (Lagrangian) is shown as a scatter of spheres whose diameter is scaled to the plot. The continuous lines delimit the boundary domain, the dashed line is the trace of the sampling plane. Different segments of the iso-surface only, from near injection to breakup, are also displayed in the three inserts.

Impinging jets - density ratio 819:1

Arienti (UTRC), Soteriou (UTRC), Sussman (FSU).

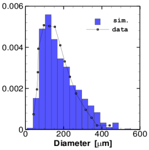

1086 samples from 5.24 to 6.58 ms

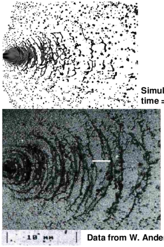

Simulation: time = 6.54 ms

Snapshot from experiment
0.64 mm-i.d., L/d$_0$=80 and 2θ =60°

Data from W. Anderson, 1995

United Technologies Research Center

Flow through diesel nozzle with moving valve

Generic mini-sac type single-hole

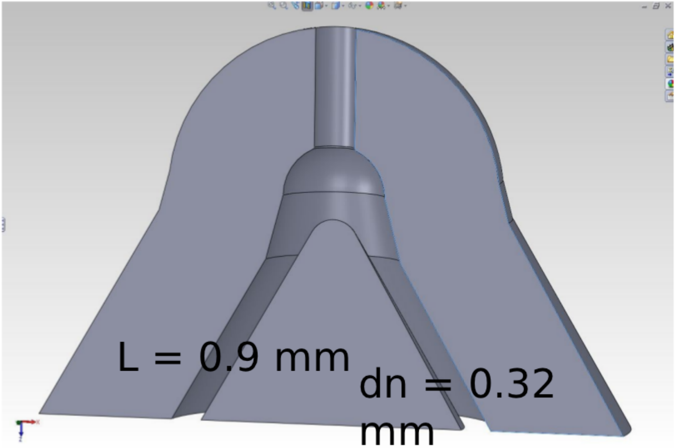

Flow through diesel nozzle with moving valve

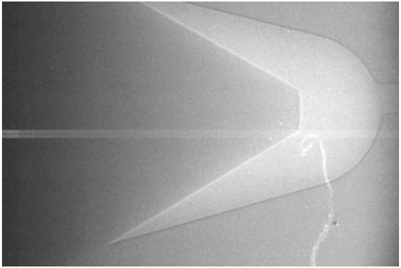

Two separate rigid bodies that can translate rigidly

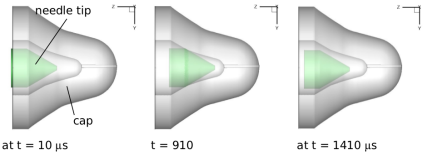

Simulation of Flow through diesel nozzle with moving valve

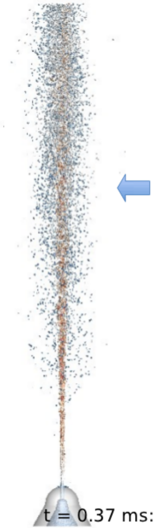

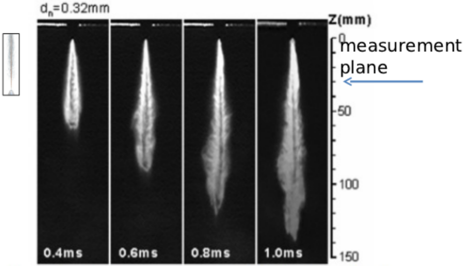

Spray images after start of injection

t = 0.37 ms: liquid surface colored by velocity from 0 to 240 m/s

AMR grid

Solid level set for fully closed passage

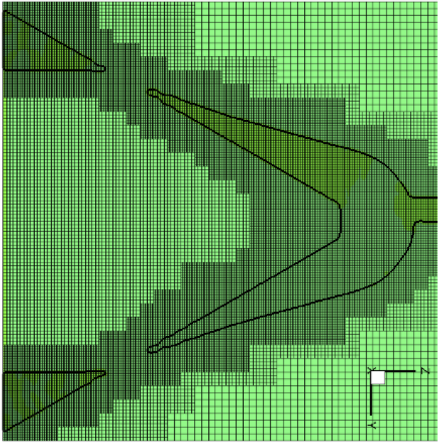

Six hole diesel nozzle

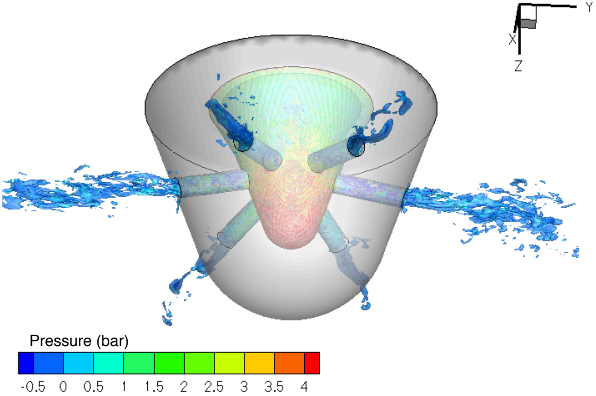

Figure: Snapshot of a simulation of liquid injection in a Bosch six-hole vertical diesel nozzle. Effective fine grid resolution 640x640x256.

Microfluidics

Sussman (FSU), Jemison (FSU), Duffy (FSU), Roper (FSU)

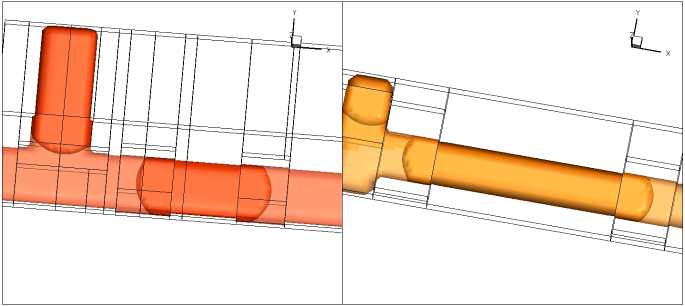

Vortex Rings

Sussman (FSU), Ohta (Tokushima)

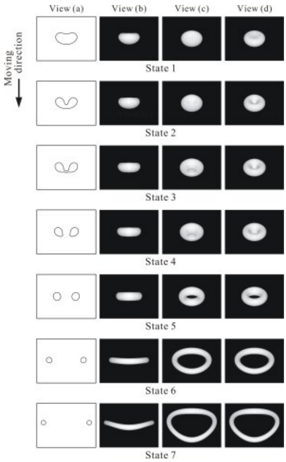

Vortex Rings

Sussman (FSU), Ohta (Tokushima)

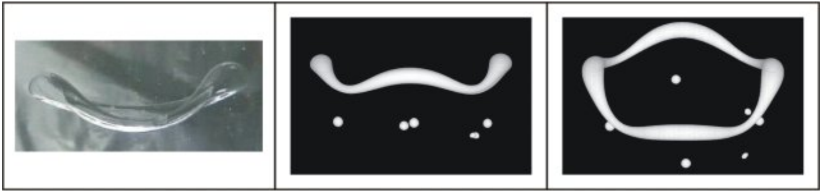

Background

- Shock capturing (ENO) - Shu, Osher, JCP 1989
- Front capturing (LS) - Sussman, Smereka, Osher, JCP 1994
- Conservative LS - Olsson, Kreiss, Zahedi, JCP 2007
- Front tracking - Unverdi, Tryggvason, JCP 1992
- VOF - Kothe, Brackbill, Zemach, JCP 1992
- CLSVOF - Sussman, Puckett; Sussman, Smith, Hussaini, et al.
- CLSVOF - Stern
- Particle LS - Enright, Fedkiw
- Refined LS - Herrmann, Pitsch

Grid

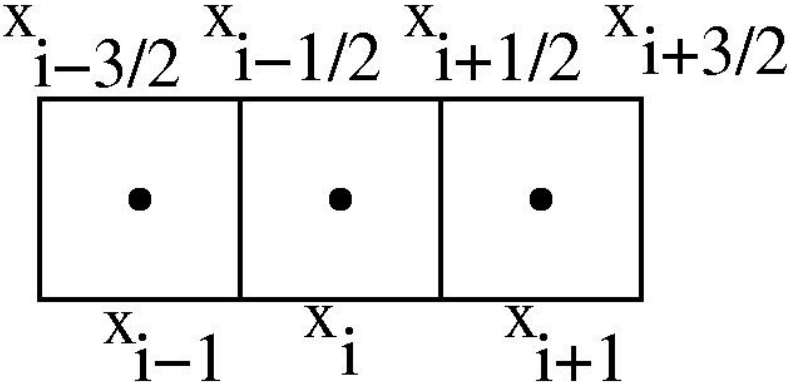

We propose Semi-Lagrangian technique for multimaterial problems, in contrast to a finite volume technique which is (in 1D, u is constant):

$$\bar{\rho}_i = \frac{1}{\Delta x} \int_{x_{i-1/2}}^{x_{i+1/2}} \rho(x) dx$$

$$\frac{d\bar{\rho}_i(t)}{dt} = -\frac{f(\rho^-_{i+1/2}, \rho^+_{i+1/2}) - f(\rho^-_{i-1/2}, \rho^+_{i-1/2})}{\Delta x}$$

where d/dt discretized using high order TVD preserving RK and $\rho_{i+1/2}$ derived from a high order ENO or WENO reconstruction.

Results motivating SL instead of Finite volume

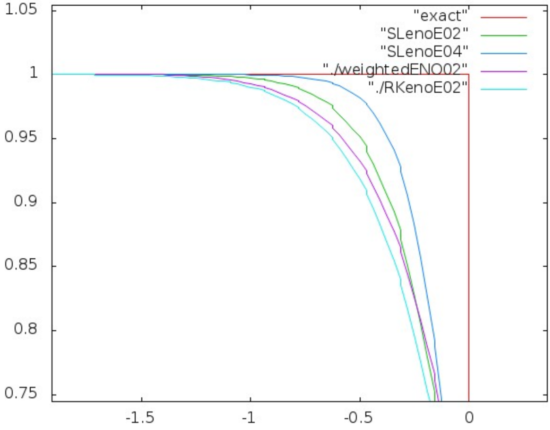

Results motivating MOF/VOF instead of ENO/WENO reconstruction

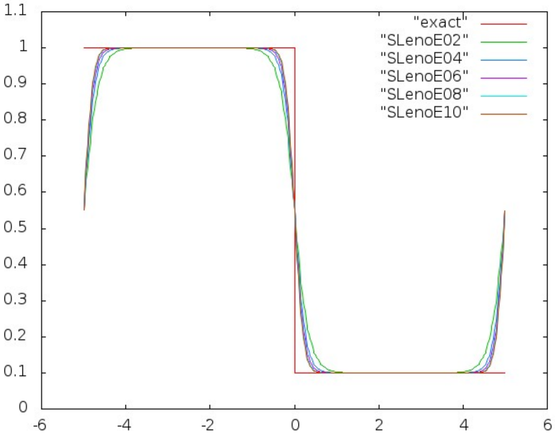

Results motivating MOF/VOF instead of ENO/WENO reconstruction

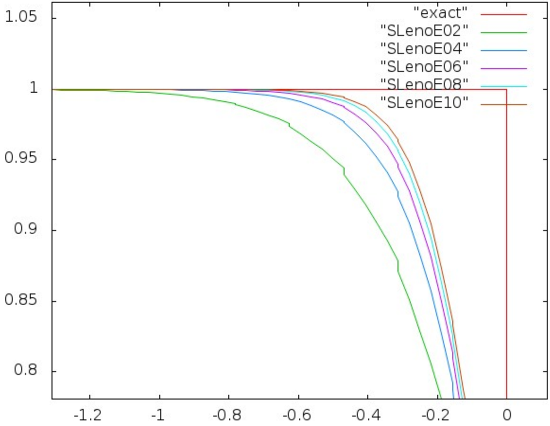

Governing Equations

$$\rho(\phi)\frac{D\mathbf{u}}{Dt} = -\nabla p + \nabla \cdot (2\mu(\phi)D) - \sigma\kappa(\phi)\nabla H(\phi) + \rho(\phi) g\hat{z}$$

$$\nabla \cdot \mathbf{u} = 0$$

$$\frac{D\phi}{Dt} = 0$$

$$H(\phi) = \begin{cases} 1 & \phi \geq 0 \\ 0 & \phi < 0 \end{cases}$$

$$\rho(\phi) = \rho_L H(\phi) + \rho_G(1 - H(\phi)),$$

$$\mu(\phi) = \mu_L H(\phi) + \mu_G(1 - H(\phi)),$$

$$\kappa(\phi) = \nabla \cdot \frac{\nabla\phi}{|\nabla\phi|},$$

$$D = \frac{\nabla\mathbf{u} + (\nabla\mathbf{u})^T}{2},$$

Splitting of advection terms from the pressure terms

Kwatra, Su, Gretarsson (JCP, 2009)

$$
\begin{aligned}
\rho_t + \nabla \cdot (\rho \mathbf{u}) &= 0 \\
(\rho \mathbf{u})_t + \nabla \cdot (\rho \mathbf{u}\mathbf{u}) &= -\nabla p \\
(\rho E)_t + \nabla \cdot (\rho \mathbf{u} E) &= -\nabla \cdot (\mathbf{u} p)
\end{aligned}
$$

Splitting of advection terms from the pressure terms

Kwatra, Su, Gretarsson (JCP, 2009)
solve the following equations to get ρ^{n+1}, $\mathbf{u}^*$, and E^*. These equations are solved using a directionally split method in which ρ at material boundaries is derived from the multimaterial MOF reconstruction.

$$\rho_t + \nabla \cdot (\rho \mathbf{u}) = 0$$
$$(\rho \mathbf{u})_t + \nabla \cdot (\rho \mathbf{u} \mathbf{u}) = 0$$
$$(\rho E)_t + \nabla \cdot (\rho \mathbf{u} E) = 0$$

Splitting of advection terms from the pressure terms

$$\frac{p^{n+1} - p^*}{\Delta t} = -\rho c^2 \nabla \cdot \mathbf{u}$$

$$\mathbf{u}^{n+1} = \mathbf{u}^* - \Delta t \frac{\nabla p}{\rho^{n+1}}$$

$$\frac{p^{n+1}}{\rho c^2 \Delta t^2} - \nabla \cdot \frac{\nabla p^{n+1}}{\rho^{n+1}} = \frac{p^*}{\rho c^2 \Delta t^2} - \frac{1}{\Delta t} \nabla \cdot \mathbf{u}^*$$

Splitting of advection terms from the pressure terms

$$u_{i+1/2}^{n+1} = u_{i+1/2}^{*} - \Delta t \frac{p_{i+1}^{n+1} - p_{i}^{n+1}}{\rho_{i+1/2}\Delta x}$$

$$u_{i}^{n+1} = u_{i}^{*} - \Delta t \frac{p_{i+1/2}^{n+1} - p_{i-1/2}^{n+1}}{\rho_{i}\Delta x}$$

$$(\rho E)^{n+1} = (\rho E)^{*} - \Delta t \nabla \cdot (\mathbf{u}^{n+1} p^{n+1})$$

CLSMOF (illustration of Piecewise linear reconstruction)

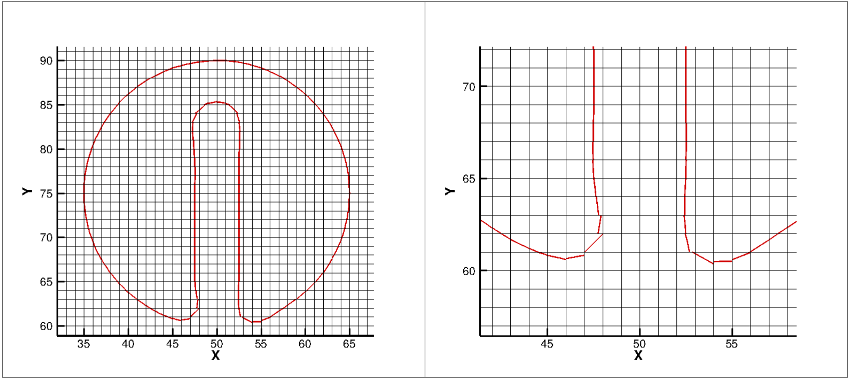

Multimaterial MOF reconstruction

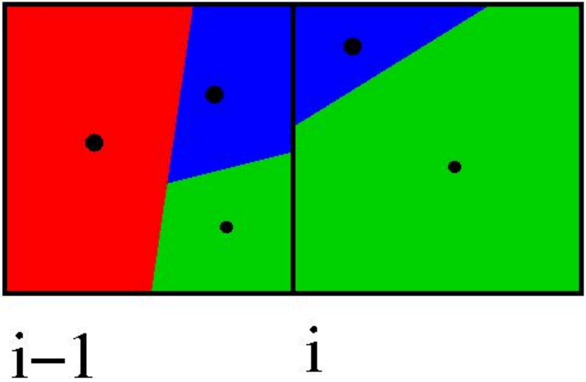

- For cell $i-1$, slope of Red (solid) cut determined first, then slope of green (fluid 1) cut determined second. Blue material occupies remaining unfilled region.
- For cell i, slope of blue (fluid 2) cut determined first. Green material occupies remaining unfilled region.

Multimaterial MOF reconstruction

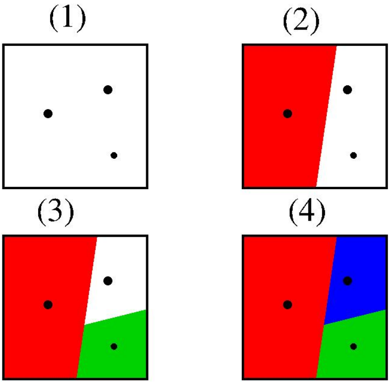

Slope of Red (solid) cut determined first, then slope of green (fluid 1) cut determined second. Blue material occupies remaining unfilled region.

MOF optimization problem

$\hat{n}$ points into the material being reconstructed. The starting guess is $\hat{n} = \frac{\mathbf{x}_{ref} - \mathbf{x}_{unfilled}}{||\mathbf{x}_{ref} - \mathbf{x}_{unfilled}||}$.

$$\{\mathbf{x} \in \mathbb{R}^3 | \hat{n} \cdot (\mathbf{x} - \mathbf{x}_{i,j,k}) + b = 0\}$$

$$|F_{\mathrm{ref}}(\hat{n}, b) - F_A(\hat{n}, b)| = 0$$

$$E_{MOF} = \|\mathbf{x}_{\mathrm{ref}} - \mathbf{x}_A(\hat{n}, b)\|_2$$

$$E_{MOF}(\Phi^*, \Theta^*) = \|f(\Phi^*, \Theta^*)\|_2 = \min_{(\Phi,\Theta)} \|f(\Phi, \Theta)\|_2,$$

$$f : \mathbb{R}^2 \rightarrow \mathbb{R}^3, \quad f(\Phi, \Theta) = (\mathbf{x}_{\mathrm{ref}} - \mathbf{x}_A(\Phi, \Theta))$$

Constrained optimization problem solved using the Gauss-Newton method.

Gauss-Newton minimization algorithm

0. initial angles: (Φ_0, Θ_0). Tolerance: $\mathrm{tol} = 10^{-8}\Delta x$.

while not converged

1. find $b_k(\Phi_k, \Theta_k)$.
2. find the centroid $\mathbf{x}_k(b_k, \Phi_k, \Theta_k)$
3. find the Jacobian matrix J_k of f evaluated in (Φ_k, Θ_k) and $f_k = f(\Phi_k, \Theta_k)$
4. stop if one of the following three conditions is fulfilled:
   - $\|J_k^T \cdot f_k\| \leq \mathrm{tol} \cdot 10^{-2}\Delta x$
   - $\|f_k\| < \mathrm{tol}$
   - $k = 11$

   else continue
5. solve the linear least squares problem: find $s_k \in \mathbb{R}^2$ such that

$$\|J_k s_k + f_k\|_2 = \min_{s \in \mathbb{R}^2} \|J_k s + f_k\|_2$$

   by means of the normal equations. $(J_k^T J_k s_k = J_k^T f_k)$
6. update the angles: $(\Phi_{k+1}, \Theta_{k+1}) = (\Phi_k, \Theta_k) + s_k$
7. $k := k + 1$

Property of MOF reconstruction

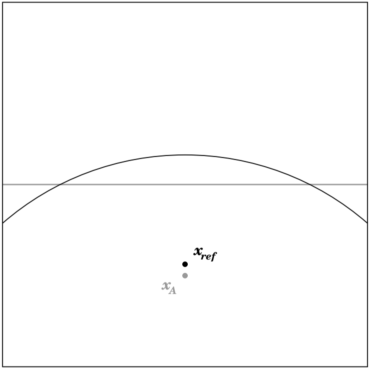

Figure: The reference centroid, $\mathbf{x}_{ref}$, does not coincide with the exact centroid, $\mathbf{x}_A$, for a parabolic interface cutting the cell. The difference between the two centroids is proportional to the curvature.

Backwards Tracing

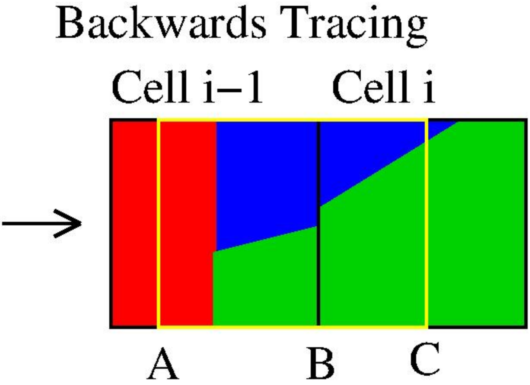

$$A = x_{i-1/2} - u_{i-1/2}\Delta t$$
$$B = x_{i-1/2}$$
$$C = x_{i+1/2} - u_{i+1/2}\Delta t$$

Backwards Tracing (before and after)

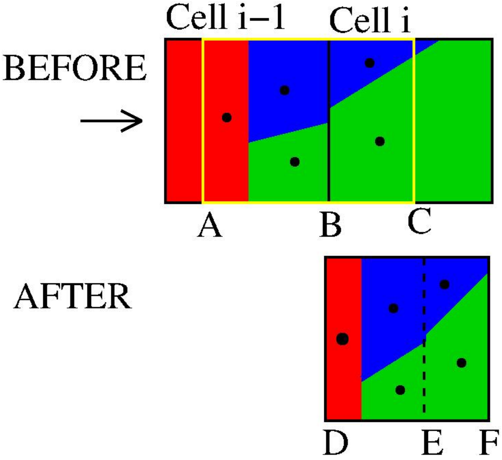

$$A = x_{i-1/2} - u_{i-1/2}\Delta t \quad B = x_{i-1/2} \quad C = x_{i+1/2} - u_{i+1/2}\Delta t$$

$$D = x_{i-1/2} \quad E = J_i(x_{i-1/2}) \quad F = x_{i+1/2}$$

Backwards Tracing - conserved variables

AKA "Eulerian Implicit"

$$\bar{\rho}_{i,j,k} = \frac{1}{\Delta x \Delta y \Delta z} \int_{x_{i-1/2}}^{x_{i+1/2}} \int_{y_{j-1/2}}^{y_{j+1/2}} \int_{z_{k-1/2}}^{z_{k+1/2}} \rho(x,y,z) dz dy dx$$

WLOG, drop j and k subscripts.

$$\bar{\rho}_i^{n+1} = \frac{\sum_{i'=i-1}^{i+1} \int_{\Omega_i^D \cap \Omega_{i'}} \rho_{i'}^n(x) dx}{\Delta x}$$

Backwards Tracing - volume fraction

AKA "Eulerian Implicit" (Scardovelli and Zaleski, Le Chenedac and Pitsch)

$$F_{i,j,k} = \frac{1}{\Delta x \Delta y \Delta z} \int_{x_{i-1/2}}^{x_{i+1/2}} \int_{y_{j-1/2}}^{y_{j+1/2}} \int_{z_{k-1/2}}^{z_{k+1/2}} H(\phi(x,y,z))dzdydx$$

$H(\phi) = 1$ if $\phi \geq 0$ (i.e. (x,y,z) inside the material being advected).

$$\phi_{i'}^{n+1} = \phi_{i'}^{n}(J_i^{-1}(x), y, z)$$

$$F_i^{n+1} = \frac{\sum_{i'=i-1}^{i+1} \int_{J_i(\Omega_i^D \cap \Omega_{i'})} H(\phi_{i'}^{n+1}(x,y,z))dxdydz}{\Delta x \Delta y \Delta z}$$

Backwards Tracing - centroid

AKA "Eulerian Implicit"

$$\mathbf{x}_{i,j,k}^{act} = \frac{1}{F_{i,j,k}\Delta x \Delta y \Delta z} \int_{x_{i-1/2}}^{x_{i+1/2}} \int_{y_{j-1/2}}^{y_{j+1/2}} \int_{z_{k-1/2}}^{z_{k+1/2}} \mathbf{x} H(\phi(x,y,z)) dz dy dx$$

$H(\phi) = 1$ if $\phi \geq 0$ (i.e. (x, y, z) inside the material being advected).

$$\phi_{i'}^{n+1} = \phi_{i'}^{n}(J_i^{-1}(x), y, z)$$

$$\mathbf{x}_i^{n+1} = \frac{\sum_{i'=i-1}^{i+1} \int_{J_i(\Omega_i^D \cap \Omega_{i'})} \mathbf{x} H(\phi_{i'}^{n+1}(x,y,z)) dx dy dz}{F_i^{n+1} \Delta x \Delta y \Delta z}$$

Backwards Tracing - mapping function

$$\Omega_i = [x_{i-1/2}, x_{i+1/2}]$$

$$\Omega_i^D = [x_{i-1/2} - u_{i-1/2}\Delta t, x_{i+1/2} - u_{i+1/2}\Delta t]$$

$$\Omega_i^T = [x_{i-1/2}, x_{i+1/2}]$$

Backwards Tracing - mapping function

Let $J_i(x) = Ax + B$ be a function which maps from cell i departure region to cell i target region. For backwards tracing,

$$J_i(x_{i-1/2} - u_{i-1/2}\Delta t) = A(x_{i-1/2} - u_{i-1/2}\Delta t) + B = x_{i-1/2}$$
$$J_i(x_{i+1/2} - u_{i+1/2}\Delta t) = A(x_{i+1/2} - u_{i+1/2}\Delta t) + B = x_{i+1/2}$$

$$A = \frac{1}{1 - (u_{i+1/2} - u_{i-1/2})\frac{\Delta t}{\Delta x}} \quad B = x_{i-1/2} - A(x_{i-1/2} - u_{i-1/2}\Delta t)$$

As long as $u\Delta t < \Delta x/2$, the mapping has an inverse.

Backwards Tracing - inverse mapping function

Let $J_i^{-1}(x)$ be the inverse map which is a function which maps from cell i target region to cell i departure region. If $J_i(x) = Ax + B$, then

$$J_i^{-1}(x) = \frac{1}{A}x - \frac{B}{A}$$

Let $\Omega^{-1} = J_i^{-1}(\Omega)$ be the inverse map which finds the region Ω^{-1} which maps to Ω under the definition of J_i. In otherwords,

$$\Omega = [a, b]$$

$$\Omega^{-1} = J_i^{-1}(\Omega) = [J_i^{-1}(a), J_i^{-1}(b)]$$

Backwards Tracing - mapping function to find target region

Likewise, $J_i(\Omega)$ is defined as the target region that the region Ω maps to:

$$\Omega = [a, b]$$
$$J_i(\Omega) = [J_i(a), J_i(b)]$$

Backwards Tracing - interface advection defined by mapping

Given a local level set function,

$$\phi_{i'}^{n}(x,y,z) = \mathbf{n}\cdot(\mathbf{x}-\mathbf{x}_{i'}) + \alpha,$$

After advection, we have

$$\phi_{i'}^{n+1}(x,y,z) = \phi_{i'}^{n}(J_i^{-1}(x),y,z) =$$
$$n_1\left(\frac{x}{A} - \frac{B}{A} - x_{i'}\right) + n_2(y-y_{j'}) + n_3(z-z_{k'}) =$$
$$\frac{n_1}{A}(x - J_i(x_{i'})) + n_2(y-y_{j'}) + n_3(z-z_{k'}) + \alpha$$

Forwards Tracing

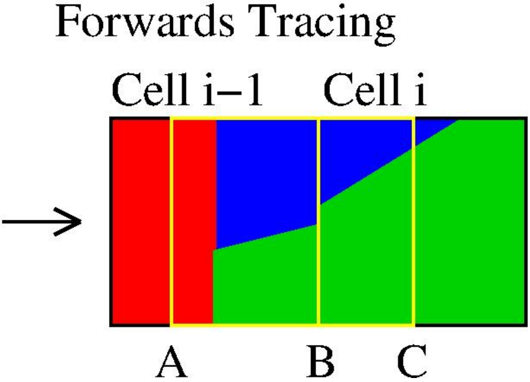

$$A = J_{i-1}^{-1}(x_{i-1/2}) \qquad B = x_{i-1/2} \qquad C = J_i^{-1}(x_{i+1/2})$$

J_{i-1} and J_i define the mappings of cells $i-1$ and i contents forward, respectively.

Forwards Tracing (before and after)

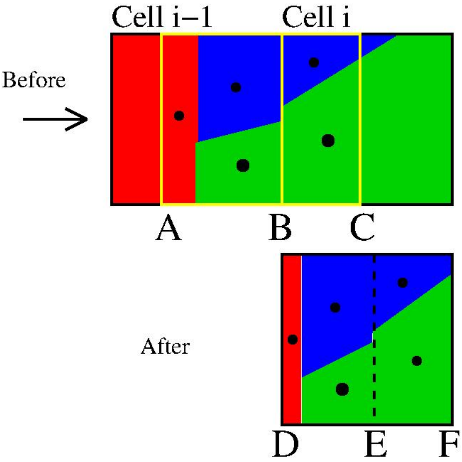

$$A = J_{i-1}^{-1}(x_{i-1/2}) \quad B = x_{i-1/2} \quad C = J_i^{-1}(x_{i+1/2})$$
$$D = x_{i-1/2} \quad E = J_i(x_{i-1/2}) \quad F = x_{i+1/2}$$

Forwards Tracing - conserved variables

AKA "Lagrangian Explicit"

$$\bar{\rho}_i = \frac{1}{\Delta x} \int_{x_{i-1/2}}^{x_{i+1/2}} \rho(x) dx$$

$$\bar{\rho}_i^{n+1} = \frac{\sum_{i'=i-1}^{i+1} \int_{J_{i'}^{-1}(\Omega_{i'}^T \cap \Omega_i)} \rho_{i'}^n(x) dx}{\Delta x}$$

Forwards Tracing - volume fraction

AKA "Lagrangian Explicit" (Scardovelli and Zaleski, Le Chenedac and Pitsch)

$$F_{i,j,k} = \frac{1}{\Delta x \Delta y \Delta z} \int_{x_{i-1/2}}^{x_{i+1/2}} \int_{y_{j-1/2}}^{y_{j+1/2}} \int_{z_{k-1/2}}^{z_{k+1/2}} H(\phi(x,y,z))dzdydx$$

$H(\phi) = 1$ if $\phi \geq 0$ (i.e. (x,y,z) inside the material being advected).

$$\phi_{i'}^{n+1}(x,y,z) = \phi_{i'}^{n}(J_{i'}^{-1}(x),y,z)$$

$$F_i^{n+1} = \frac{\sum_{i'=i-1}^{i+1} \int_{\Omega_i \cap \Omega_{i'}^T} H(\phi_{i'}^{n+1}(x,y,z))dxdydz}{\Delta x \Delta y \Delta z}$$

Forwards Tracing - centroid

AKA "Lagrangian Explicit"

$$\mathbf{x}^{act}_{i,j,k} = \frac{1}{F_{i,j,k}\Delta x \Delta y \Delta z} \int_{x_{i-1/2}}^{x_{i+1/2}} \int_{y_{j-1/2}}^{y_{j+1/2}} \int_{z_{k-1/2}}^{z_{k+1/2}} \mathbf{x} H(\phi(x,y,z)) dz dy dx$$

$H(\phi) = 1$ if $\phi \geq 0$ (i.e. (x,y,z) inside the material being advected).

$$\phi^{n+1}_{i'}(x,y,z) = \phi^{n}_{i'}(J^{-1}_{i'}(x), y, z)$$

$$\mathbf{x}^{n+1}_{i} = \frac{\sum_{i'=i-1}^{i+1} \int_{\Omega_i \cap \Omega^T_{i'}} \mathbf{x} H(\phi^{n+1}_{i'}(x,y,z)) dx dy dz}{F^{n+1}_{i} \Delta x \Delta y \Delta z}$$

Forwards Tracing - mapping function

$$\Omega_i = [x_{i-1/2}, x_{i+1/2}]$$

$$\Omega_i^T = [x_{i-1/2} + u_{i-1/2}\Delta t, x_{i+1/2} + u_{i+1/2}\Delta t]$$

$$\Omega_i^D = [x_{i-1/2}, x_{i+1/2}]$$

Forwards Tracing - mapping function

Let $J_i(x) = Ax + B$ be a function which maps from cell i departure region to cell i target region. For forwards tracing,

$$J_i(x_{i-1/2}) = Ax_{i-1/2} + B = x_{i-1/2} + u_{i-1/2}\Delta t$$
$$J_i(x_{i+1/2}) = Ax_{i+1/2} + B = x_{i+1/2} + u_{i+1/2}\Delta t$$

$$A = 1 + (u_{i+1/2} - u_{i-1/2})\frac{\Delta t}{\Delta x} \quad B = x_{i-1/2} + u_{i-1/2}\Delta t - Ax_{i-1/2}$$

As long as $u\Delta t < \Delta x/2$, A is positive.

Forwards Tracing - inverse mapping function

Let $J_i^{-1}(x)$ be the inverse map which is a function which maps from cell i target region to cell i departure region. If $J_i(x) = Ax + B$, then

$$J_i^{-1}(x) = \frac{1}{A}x - \frac{B}{A}$$

Let $\Omega^{-1} = J_i^{-1}(\Omega)$ be the inverse map which finds the region Ω^{-1} which maps to Ω under the definition of J_i. In otherwords,

$$\Omega = [a, b]$$
$$\Omega^{-1} = J_i^{-1}(\Omega) = [J_i^{-1}(a), J_i^{-1}(b)]$$

Forwards Tracing - mapping function to find target region

Likewise, $J_i(\Omega)$ is defined as the target region that the region Ω maps to:

$$\Omega = [a, b]$$
$$J_i(\Omega) = [J_i(a), J_i(b)]$$

Forwards Tracing - advection of interface reconstruction by defined mapping

Given a local level set function,

$$\phi_{i'}^{n}(x,y,z) = \mathbf{n}\cdot(\mathbf{x}-\mathbf{x}_{i'}) + \alpha,$$

After forward advection, we have

$$\phi_{i'}^{n+1}(x,y,z) = \phi_{i'}^{n}(J_{i'}^{-1}(x),y,z) =$$
$$n_1(\frac{x}{A}-\frac{B}{A}-x_{i'}) + n_2(y-y_{j'}) + n_3(z-z_{k'}) =$$
$$\frac{n_1}{A}(x-J_{i'}(x_{i'})) + n_2(y-y_{j'}) + n_3(z-z_{k'}) + \alpha$$

DS Semi-Lagrangian discretization - Strang Splitting

1. x direction; backwards projection. (Eulerian Implicit)
2. y direction; forwards projection. (Lagrangian Explicit)
3. z direction; backwards projection. (Eulerian Implicit)
4. z direction; forwards projection. (Lagrangian Explicit)
5. y direction; backwards projection. (Eulerian Implicit)
6. x direction; forwards projection. (Lagrangian Explicit)

2D volume conserved exactly

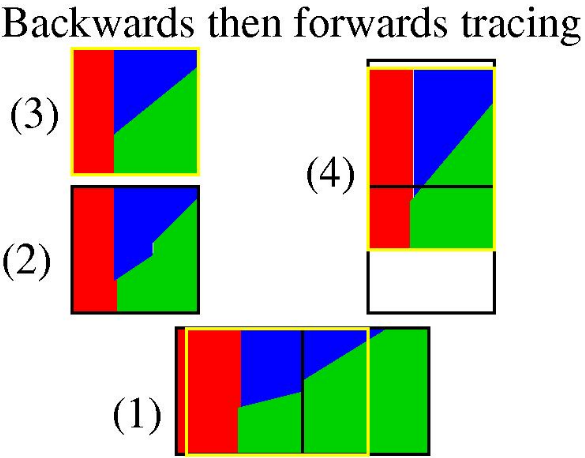

reversible single vortex

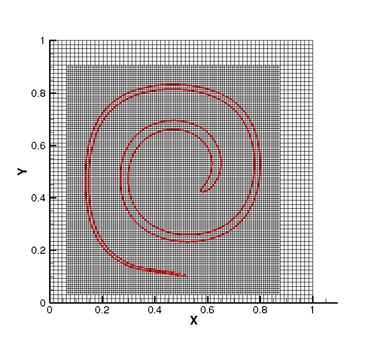

2D Unsplit MOF, reversible vortex T=1/2

RK2, backwards tracing:

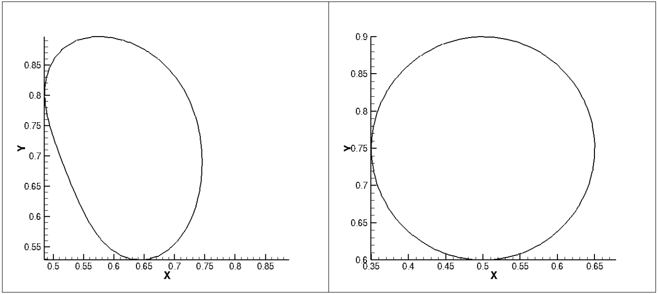

Figure: single vortex problem ($T = 1/2$) 64×64 midway through the simulation and at the end. Shape deforms back to a circle. Two materials. At $t = T = 1/2$, symmetric difference error is $7.4E - 5$ (operator split symmetric difference error: $14.3E - 5$)

2D Unsplit multimaterial MOF, reversible vortex T=1/2

RK2, backwards tracing:

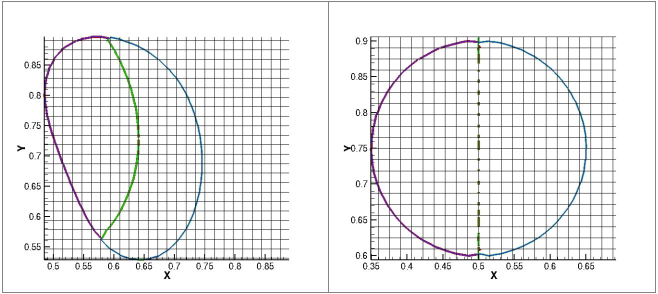

Figure: single vortex problem ($T = 1/2$) 64×64 midway through the simulation and at the end. Shape deforms back to a circle. Three materials. Initially, Material 1 (red) is the left half of the circle, Material 2 (green) is the right half, and Material 3 (blue) is the space outside the circle. At $t = T = 1/2$, symmetric difference error is $9.6E-5$ for material 1, $10.1E-5$ for material 2, and $14.8E-5$ for material 3.

3D Unsplit MOF, reversible vortex T=3

RK2, backwards tracing:

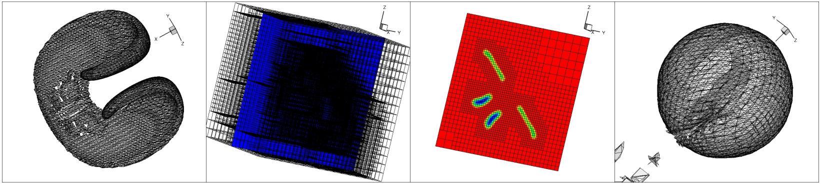

Figure: 3D single vortex problem ($T = 3$) $64 \times 64 \times 64$ midway through the simulation and at the end. Shape deforms back to a sphere. Two materials. At $t = T = 3$, symmetric difference error is 0.00189 (operator split symmetric difference error: 0.00202)

3D Unsplit multimaterial MOF, reversible vortex T=3

RK2, backwards tracing:

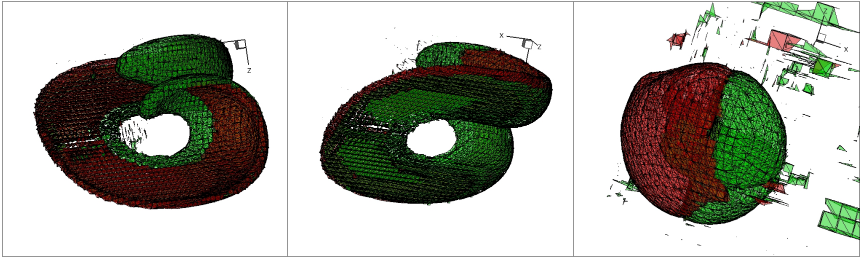

Figure: single vortex problem ($T = 3$) $64 \times 64 \times 64$ midway through the simulation and at the end. Shape deforms back to a sphere. Three materials. Initially, Material 1 (red) is the left half of the sphere, and Material 2 (green) is the right half. At $t = T = 3$, symmetric difference error is 0.00158 for material 1, 0.00104 for material 2, and 0.00188 for material 3.

Rotating Notched disk (Zalesak's problem)

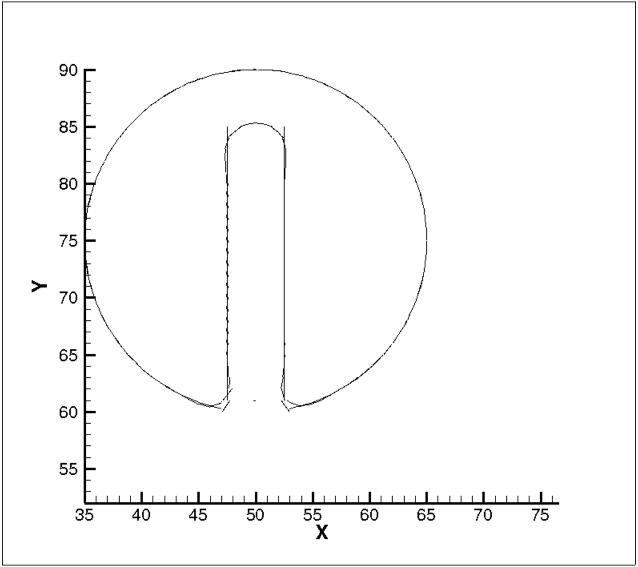

Rotating Letter “A”

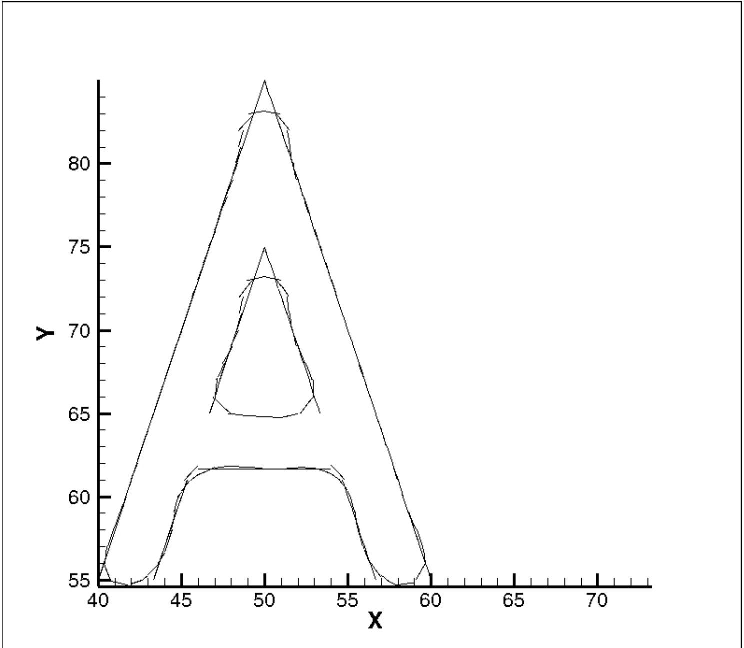

Rising gas bubble in liquid

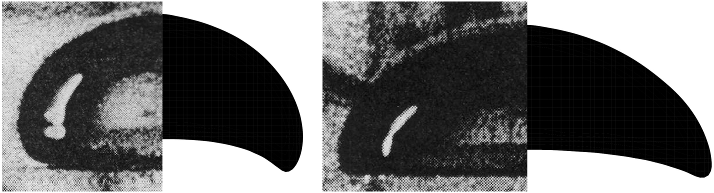

Figure: Left: condition 1 Right: condition 3

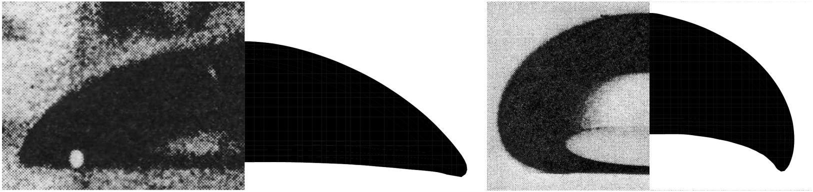

Figure: Left: condition 4 Right: condition 6

Surface tension driven vibrations of a drop

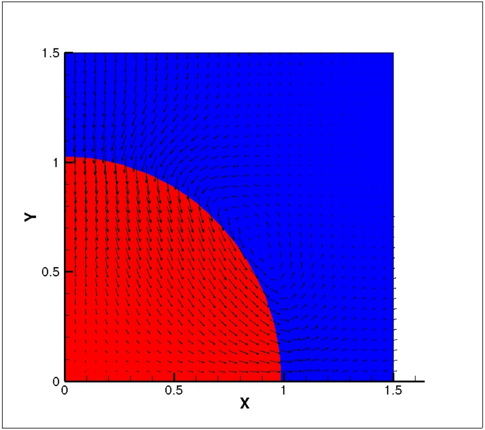

Oscillating Cylinder

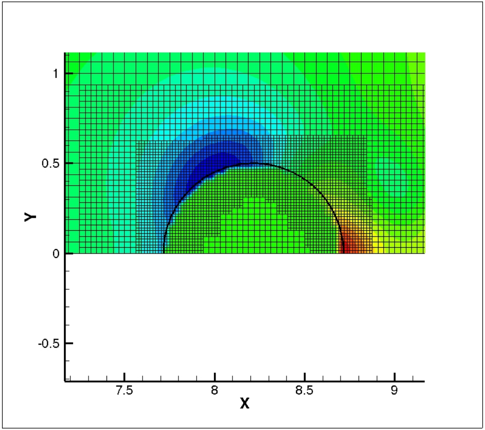

Cylinder falling into a pool of liquid

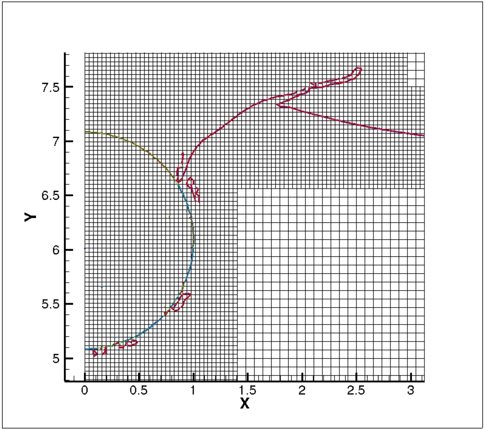

Impinging jets - same material

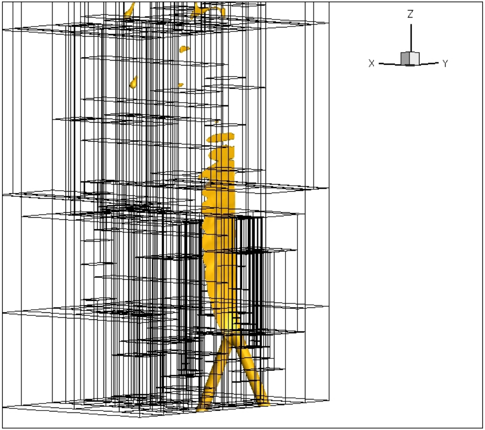

Impinging jets - different materials

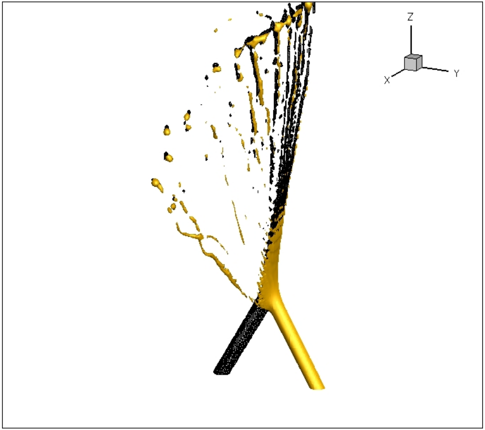

Future work

The multimaterial MOF representation enables more accurate simulation of:

- multimaterial flows with minimal volume fluctuation - capturing corners and filaments.
- surface tension and contact line effects.
- simulating transport on deforming surfaces.
- predicting mass transfer on deforming surfaces.
- predicting boundary layer effects on underresolved grids.

Improvements are still being made to the multimaterial MOF scheme in accelerating the multimaterial MOF reconstruction and unsplit multimaterial MOF advection algorithm. Adding the capability to robustly simulate compressible multiphase/multimaterial flows is one priority now.